Proliferation-promoting roles of linear and circular PVT1 are independent of their ability to bind miRNAs in B-cell lymphoma

Zhao, Xing; van den Berg, Anke; Winkle, Melanie; Koerts, Jasper; Seitz, Annika; de Jong, Debora; Rutgers, Bea; van der Sluis, Tineke; Bakker, Emke; Kluiver, Joost

Published in:
International Journal of Biological Macromolecules

DOI:
10.1016/j.ijbiomac.2023.126744

Publication date:
2023

International Journal of Biological Macromolecules 253 (2023) 126744

Contents lists available at ScienceDirect

International Journal of Biological Macromolecules

journal homepage: www.elsevier.com/locate/ijbiomac

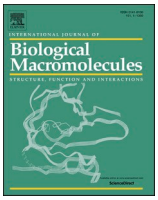

Proliferation-promoting roles of linear and circular PVT1 are independent of their ability to bind miRNAs in B-cell lymphoma

Xing Zhao, Anke van den Berg *, Melanie Winkle, Jasper Koerts, Annika Seitz, Debora de Jong, Bea Rutgers, Tineke van der Sluis, Emke Bakker, Joost Kluiver *

Department of Pathology and Medical Biology, University of Groningen, University Medical Center Groningen, 9700 RB Groningen, the Netherlands

ARTICLE INFO

Keywords:
PVT1
circPVT1
B-cell lymphoma

ABSTRACT

Plasmacytoma Variant Translocation 1 (PVT1) is a long non-coding RNA located at 8q24.21 immediately downstream of MYC. Both the linear and circular PVT1 transcripts contribute to cancer pathogenesis by binding microRNAs. However, little is known about their roles in B-cell lymphoma. Here we studied their expression patterns, role in growth, and ability to bind miRNAs in B-cell lymphoma. Linear PVT1 transcripts were down-regulated in B-cell cell lymphoma lines compared to germinal center B cells, while circPVT1 levels were increased. Two Hodgkin lymphoma cell lines had a homozygous deletion including the 5′ region of the PVT1 locus, resulting in a complete lack of circPVT1 and 5′ linear PVT1 transcripts. Inhibition of both linear and circular PVT1 decreased growth of Burkitt lymphoma, while the effects on Hodgkin lymphoma and diffuse large B cell lymphoma were less pronounced. Overexpression of circPVT1 promoted growth of B-cell lymphoma lacking or having low endogenous circPVT1 levels. Contrary to other types of cancer, linear and circular PVT1 transcripts did not interact with miRNAs in B-cell lymphoma. Overall, we showed an opposite expression pattern of linear and circular PVT1 in B-cell lymphoma. Their effect on growth was independent of their ability to bind miRNAs.

1. Introduction

In contrast to the small proportion of the human genome that encodes protein-coding transcripts, >60 % of the genome is transcribed into RNA molecules that are not translated into proteins. These RNAs belong to the family of non-coding (nc) RNAs [1–3]. NcRNAs are broadly subdivided into small and long ncRNAs (lncRNAs) based on an arbitrary cutoff of 200 nucleotides [2]. Unlike protein-coding genes, lncRNAs have a lower abundance, a more pronounced tissue-specific expression pattern, limited sequence conservation, and more variable subcellular localization patterns [4]. Functionally, lncRNAs are involved in regulation of gene transcription, RNA processing, translation, and epigenetic modifications through interaction with DNA, RNA, and proteins [5–7]. Recently, a relatively new subgroup of ncRNAs was defined, i.e., circular RNAs (circRNAs) [8,9]. CircRNAs have a closed loop shape without 5′ and 3′ ends [10] that is formed by back-splicing or exon skipping [11]. The circular shape leads to highly stable transcripts that are in general resistant to RNase R digestion [12]. Most circRNAs are derived from protein-coding genes and exhibit tissue-specific expression patterns [9,13]. Depending on their subcellular localization, circRNAs can regulate gene transcription and alternative splicing, stabilize mRNAs, serve as microRNA decoys, act as protein sponges or scaffolds, and serve as templates for translation [8,14]. Although many lncRNAs and circRNAs have been identified, most of them still need to be functionally characterized. Despite the overall limited knowledge of functionality, it has become clear that circRNAs can play key roles in the pathogenesis of a variety of diseases and malignancies [8,9].

The Plasmacytoma Variant Translocation 1 (PVT1) locus is located at 8q24.21, about 53 kb downstream of the well-known *MYC* proto-oncogene locus [15]. In addition to harboring two fragile sites (FRA8C and FRA8D), the PVT1 locus gives rise to 190 linear splicing variants (Ensembl V110), 29 circular RNAs (circBase) and five highly conserved miRNAs [16–18]. In recent years, a total of 98 different lncPVT1 fusion genes/transcripts have been identified in both hematological and solid malignancies, in line with the important role of this locus in cancer [19]. Functional research on the lncRNA PVT1 (lncPVT1) and the most

* Corresponding authors at: Department of Pathology and Medical Biology, University Medical Center Groningen, Hanzeplein 1, 9700 RB Groningen, the Netherlands.

E-mail addresses: a.van.den.berg01@umcg.nl (A. van den Berg), j.l.kluiver@umcg.nl (J. Kluiver).

https://doi.org/10.1016/j.ijbiomac.2023.126744
Received 3 May 2023; Received in revised form 1 August 2023; Accepted 27 August 2023
Available online 9 September 2023

extensively investigated circular PVT1 (circPVT1) hsa_circ_00001821 transcripts from the PVT1 locus has revealed their involvement in the pathogenesis of various malignancies [20–24]. Both lncPVT1 and circPVT1 were shown to serve as miRNA decoys and thereby attenuate the action of the corresponding miRNA on its target mRNAs [16,25,26]. Mechanistically, it has been shown that lncPVT1 interacts with c-Myc which results in a positive feedback loop to enhance their expression and promote tumorigenesis [27]. A regulatory mechanism that seems in contrast with this is that the PVT1 promoter regulates the pause release of MYC transcription by competing with the MYC promoter for four intragenic enhancers located in the PVT1 locus [28]. Deletions of the PVT1 promoter were observed among double-hit signature diffuse large B cell lymphoma (DLBCL) lacking MYC translocations [29]. Moreover, high expression of lncPVT1 predicted poor prognosis and facilitated proliferation of DLBCL cell lines [30,31]. Knockdown of lncPVT1 inhibited proliferation of the Burkitt lymphoma (BL) cell line Raji through regulating cell cycle progression [32]. Elevated levels of MYC, lncPVT1 and circPVT1 were observed in a vincristine-resistant DLBCL cell line with an amplification encompassing the MYC-PVT1 region [33]. c-Myc was shown to enhance expression of circPVT1 in the P493–6 B-cell model, supporting a link between these two factors in B cells [34]. In nasopharyngeal carcinoma, binding of circPVT1 to β-TrCP blocked binding of β-TrCP to c-Myc and this prevented proteasomal degradation of c-Myc [24]. In acute lymphoblastic leukemia, circPVT1 was shown to regulate c-Myc but the mechanism underlying this observation is unknown [35].

Here, we studied the expression of lncPVT1 and circPVT1 transcripts in a panel of B-cell lymphoma cell lines and normal B-cell subsets. In addition, we investigated the functional relevance of both PVT1 transcripts for supporting growth of B-cell lymphoma and explored their interaction with miRNAs.

2. Methods

2.1. Cell lines and isolation of B cell subsets

We used 9 Burkitt lymphoma (BL), 8 Hodgkin lymphoma (HL), and 12 diffuse large B-cell lymphoma (DLBCL) cell lines for expression profiling and a subset of the cell lines for functional studies. HEK293T cells were used for production of lentiviral particles. Details of the cell lines including EBV (Epstein Barr Virus) status, presence of MYC translocations, and culture medium are shown in Supplementary Table 1. Cells were cultured at 37 °C with 5 % CO2 in culture media supplemented with 100 U/ml penicillin, 100 μg/ml streptomycin, 2 mM UltraGlutamine, and 10 % or 20 % Fetal Bovine Serum (Sigma, St. Louis, MO, USA). All cell lines were regularly subjected to STR analysis to confirm the origin of cell lines and tested for mycoplasma. B-cell subsets were sorted from four tonsil specimens of children as described previously [36]. Written permission to use tonsil tissue was obtained from the parents of the children. The research protocol complies with international ethical guidelines (the Declaration of Helsinki and the International Conference on Harmonization Guidelines for Good Clinical Practice).

2.2. RNA isolation and reverse transcription quantitative PCR (RT-qPCR)

RNA isolation was performed using Phase Lock Gel Heavy tubes (5 Prime) in combination with the miRNeasy mini or micro kit including an on-column DNase digestion (Qiagen, Hilden, Germany) following the manufacturer's instructions. The concentration was measured using NanoDrop™ 1000 Spectrophotometer (Thermo Fisher, Waltham, MA, USA). cDNA was synthesized using SuperScript™ II Reverse Transcriptase kit (Invitrogen, Waltham, MA, USA) with 300 ng Random Primers and 500 ng RNA in a final reaction volume of 20 μl. Samples were amplified in triplicate using 1 ng cDNA and 3 μM primers in a reaction volume of 10 μl containing SYBR Green (Applied Biosystems, Waltham, MA, USA) following the protocol of the manufacturer on the Lightcycler 480 (Roche, Basel, Switzerland). Relative expression levels are shown as $2^{-\Delta Cp}$ or $2^{-\Delta\Delta Cp}$ as indicated in the figures, using TBP as a housekeeping gene. Divergent primers in exon 6 of the PVT1 exon summary locus view, which corresponds to exon 2 of PVT1 transcript NR_003367.3, were used to specifically amplify the circPVT1 transcripts (Supplementary Fig. 1). The sequences of all qPCR primers used in this study are listed in Supplementary Table 2. RT-qPCR for miRNAs was performed as described previously [37]. In brief, miRNA-specific cDNA synthesis was performed using the TaqMan MicroRNA Reverse Transcription Kit (Applied Biosystems) following a multiplex protocol. Quantitative PCR was done using 30 times diluted cDNA and TaqMan MicroRNA Assays (miR-15a-5p, assay ID: 477858_mir; miR-16-5p, assay ID: 477860_mir; and miR-17-5p, assay ID: 478447_mir; Applied Biosystems).

2.3. DNA extraction and polymerase chain reaction (PCR)

Genomic DNA was isolated using salt-chloroform-based extraction protocol. DNA concentration was measured by a NanoDrop™ 1000 Spectrophotometer and the quality was assessed by performing a ladder PCR [38]. PCR reactions were carried out using Taq DNA polymerase (Invitrogen), 10 μM PCR primers (Supplementary Table 2), and a DNA input of 100 ng using protocols as provided by the manufacturer. PCR products were analyzed on 1 % agarose gel.

2.4. RNase R treatment

Total RNA (1 μg/reaction) was incubated for 15 min at 37 °C without or with 1 U RNase R (Biosearch Technologies, Hoddesdon, UK) in a 15 μl volume. After incubation, RNA was purified and concentrated using Vivacon® 500 Hydrosart filter (Sartorius, Göttingen, Germany). To enable a direct comparison of Cp values, the volume of all tubes was restored to 15 μl. RNA integrity was assessed on a 1 % agarose gel. Subsequently, reverse transcription was performed on 10 μl of RNA and 2.5 μl of the cDNA was used for qPCR after dilution of the cDNA 62.5 times. Abundance of circular RNA was determined using primers flanking the back-splice junction (BSJ) of the circular RNA. As a control for the efficiency of the RNase R treatment, we also analyzed abundance of linear transcripts TBP and HPRT and the circRNA circ_0000284.

2.5. GFP competition assays

ShRNAs against lncPVT1 and the BSJ region of circPVT1 were designed and cloned into the miRZIP lentiviral vector (System Biosciences, Palo Alto, CA, USA) (Supplementary Table 2). Two non-targeting shRNAs (NT1 and NT2) were used as negative controls. A circPVT1 overexpression and a negative control (NC) construct were purchased from Geneseed (Guangzhou, China). Production of lentiviral particles and infection of cells was performed as described previously [37]. To determine efficiency of knockdown and overexpression, infected cells were selected by puromycin treatment for 4 days to reach a GFP-positive cell fraction of >90 %. Cells were harvested for RNA isolation and RT-qPCR. To determine the potential effect of knockdown of lncPVT1 and circPVT1 and overexpression of circPVT1 on growth, we infected cells aiming at a percentage of GFP+ cells ranging between 20 % to 60 %. The percentage of GFP+ cells was measured tri-weekly for 3 weeks starting on day 4 post-infection. The relative GFP+ percentage was determined by normalization to the GFP+ cell percentage measured on day 4. All GFP competition assays were performed in triplicate.

2.6. Isolation of cytoplasmic and nuclear fractions

A total of 0.5 million cells were harvested at 1000 x g for 5 min and resuspended in 250 μl wash buffer (10 mM Tris-HCl pH 8.0, 300 mM sucrose, 10 mM NaCl, 2 mM MgAc2, 0.5 mM DTT). The cells were lysed by adding 250 μl 2× lysis buffer (10 mM Tris-HCl pH 8.0, 300 mM

sucrose, 10 mM NaCl, 2 mM MgAc2, 6 mM CaCl2, 0.2 % Nonidet P-40, 0.5 mM DTT) and centrifuged at 1000 xg for 5 min at 4 °C The supernatant was collected as the cytoplasmic fraction. The pellet was resuspended in 0.5 ml glycerol buffer (50 mM Tris-HCl pH 8.0, 25 % glycerol, 5 mM MgAc2, 0.1 mM EDTA, 5 mM DTT) and centrifuged at 1000 xg for 5 min. The pellet was collected as the nuclear fraction. All buffers were supplemented with fresh 4 U/ml SUPERase In™ RNase Inhibitor (Invitrogen) and 1× cOmplete™ EDTA-free protease inhibitor cocktail (Merk, Kenilworth, NJ, USA). RNA was isolated using Qiazol lysis reagent (Qiagen) following the protocol of the manufacturer. RNA was eluted in 25 μl RNAse-free H2O and 1 μl RNA was used for cDNA synthesis in a volume of 20 μl. We used an input of 2.5 μl of cDNA (62.5× diluted) for qPCR. To evaluate the efficiency of the subcellular fractionation, we analyzed the levels of U3 and SNHG4 as nuclear controls, and the levels of RPPH1 as cytoplasmic control in both fractions.

2.7. AGO2 RNA immunoprecipitation (AGO2-RIP)

AGO2 RNA immunoprecipitation was performed as described previously [39]. In brief, AGO2 (Clone 2E12-1C9, Abnova, Taiwan) and IgG control (Millipore 12–371, Millipore BV, Amsterdam, The Netherlands) antibodies were incubated with EZview protein G beads (Merck) overnight at 4 °C. Next, the antibody/beads complexes were incubated with the cell lysates overnight at 4 °C. After washing, RNA was isolated using Qiazol (Qiagen). RT-qPCR was performed using equal fractions as input. Western blot of AGO2 protein in total fraction (TF), flow-through (FT), and IP fraction and RT-qPCR of miR-15a-5p, miR-16-5p, and miR-17-5p in the AGO2-IP and IgG-IP fraction were performed to evaluate the efficiency of the pulldown. Relative enrichment was calculated by $2^{-\Delta Cp}$ where ΔCp = Cp (AGO2-IP) – Cp (IgG-IP).

2.8. Statistical analysis

Differences in lncPVT1 and circPVT1 transcript levels between lymphoma cell lines and normal B cells were determined using Brown-Forsythe and Welch ANOVA tests test in GraphPad Prism (8.4.2 version, Dotmatics, San Diego, CA, USA). Significance of changes in GFP+ cell percentages in knockdown or overexpression GFP competition assays relative to controls were assessed using a Mix model analysis in IBM SPSS Statistics (28.0 version, IBM, Chicago, IL, USA) [40]. A correlation between MYC and lncPVT1 or circPVT1 transcripts was assessed by calculating the Pearson correlation coefficient (r). The correlation was defined as strong ($|r| > 0.7$), moderate ($0.7 \leq |r| < 0.5$), fair ($0.5 \leq |r| \leq 0.3$), or poor ($|r| < 0.3$). A p-value of <0.05 was considered significantly different.

3. Results

3.1. Contrasting differential expression patterns of linear and circular PVT1 transcripts

To investigate the expression patterns of lncPVT1 and circPVT1 transcripts, we examined their expression levels in a panel of 29 lymphoma cell lines (HL = 8, BL = 9, DLBCL = 12) and normal B-cell subsets by RT-qPCR. We used two different primer sets to test expression of lncPVT1, i.e., one primer set amplifying lncPVT1 transcripts containing exons 6–8 and a second primer set amplifying transcripts including exons 13–14 (exon numbering based on PVT1 exon summary view, Supplementary Fig. 1). The levels of the lncPVT1 exon 6–8 and exon 13–14 amplicons were significantly higher in normal germinal center (GC) B and memory cells as compared to naïve B cells (Supplementary Fig. 2A-B). In comparison to GC B cells, a significant downregulation of the exon 6–8 amplicon was observed in all 3 B-cell lymphoma subtypes. The exon 13–14 amplicon also showed a significant downregulation in BL, while the decreases in HL and DLBCL were not significant. The exon 6–8 amplicon was completely absent in the KM-H2 and SUPHD1 HL cell lines and the RI-1 DLBCL cell line (Fig. 1 A-B; Supplementary Fig. 3A).

The circular shape of circPVT1 was confirmed by RT-qPCR of RNA samples pre-treated with RNase R which digests linear mRNAs but not circRNAs. RNase R treatment efficiency was confirmed by the decrease in the abundance of two linear transcripts (TBP and HPRT), while the levels of the control circRNA were not affected. CircPVT1 levels were not affected by the RNase R treatment, confirming the circular shape of circPVT1 (Supplementary Fig. 4). Similar to the lncPVT1 amplicons, circPVT1 levels were higher in GC B and memory cells compared to naïve B cells, but this difference was significant only for GC B cells (Supplementary Fig. 2C). In contrast to the decreased levels observed for both lncPVT1 amplicons, expression levels of circPVT1 were increased in all B-cell lymphoma subtypes compared to GC B cells, albeit significant only in BL and DLBCL cell lines. Consistent with the absence of the exon 6–8 amplicon of lncPVT1, we also could not detect circPVT1 in KM-H2 and SUPHD1. In RI-1, the 3rd cell line that lacked the exon 6–8 amplicon of lncPVT1, we did observe expression of circPVT1 (Fig. 1C; Supplementary Fig. 3C). These results demonstrate that the expression of lncPVT1 and circPVT1 have opposite patterns in B-cell lymphoma suggesting specific regulatory mechanisms for lncPVT1 and circPVT1.

Two independent regulatory mechanisms have been reported on the dependency of PVT1 and MYC expression [28,41]. To establish potential associations in B-cell lymphoma, we correlated expression of MYC with the expression levels of lncPVT1 and circPVT1. The exon 6–8 ($r = 0.4$, $p < 0.05$) and exon 13–14 ($r = 0.48$, $p < 0.01$) amplicons of lncPVT1 showed a fair correlation with MYC levels (Supplementary Fig. 5A). The association was most obvious in MYC translocation negative cell lines (lncPVT1 exon 6–8: $r = 0.43$, $p = 0.09$; lncPVT1 exon 13–14: $r = 0.54$, $p < 0.05$) and was absent in cell lines with a MYC translocation (lncPVT1 exon 6–8: $r = -0.06$; lncPVT1 exon 13–14: $r = 0.03$) (Supplementary Fig. 5B-C). CircPVT1 showed a similar pattern, though not statistically significant (Supplementary Fig. 5). Thus, a potential regulatory link between MYC and PVT1, might be restricted to MYC translocation negative cell lines.

3.2. Homozygous deletion of the 5′ region of the PVT1 locus in two HL cell lines

To explain the lack of the lncPVT1 transcripts containing exon 6–8 and the circPVT1 transcript in three and two of the lymphoma cell lines, respectively, we analyzed the 5′ region of the PVT1 locus at the genomic level. DNA primer sets were designed to verify presence of the PVT1 exons and enhancer regions [28]. In addition, multiple RNA primer sets were designed for RT-qPCR to establish presence of the most common PVT1 splice variants (Fig. 2). For KM-H2 cells, primer sets covering a region from exons 1 to 6 up to the 912E enhancer failed to give PCR products, indicating a homozygous deleted region of the 5′ region of the PVT1 locus. In SUPHD1 cells, we observed a similar but slightly shorter homozygous deleted region, which included exons 1 to 6 but not the 912E enhancer. For both cell lines, results at the genomic level were consistent with the results obtained at the RNA level and explained the inability to detect lncPVT1 transcripts that include (part) of the deleted exons and the circPVT1 transcripts. In contrast to the HL cell lines, we did observe PCR products of the expected sizes for all genomic amplicons within the PVT1 locus in RI-1 cells. Nonetheless, we were not able to detect transcripts containing exons 6–8 and exons 5–8, while we could detect transcripts containing exons 1–2, exons 1–5, exons 5–6, exons 8–10, exons 13–14, and circPVT1 transcripts. The two cell lines included as controls, i.e., DG75 and L428, showed the expected pattern for all tested amplicons at the DNA and RNA level. Collectively, our data show a homozygous deletion of the 5' PVT1 region in KM-H2 and SUPHD1 encompassing the first 6 exons and two or three of the enhancer regions. In contrast, the lack of lncPVT1 transcripts containing exon 6–8 or exon 5–8 in RI-1 cells suggests aberrant splicing as the most likely underlying mechanism.

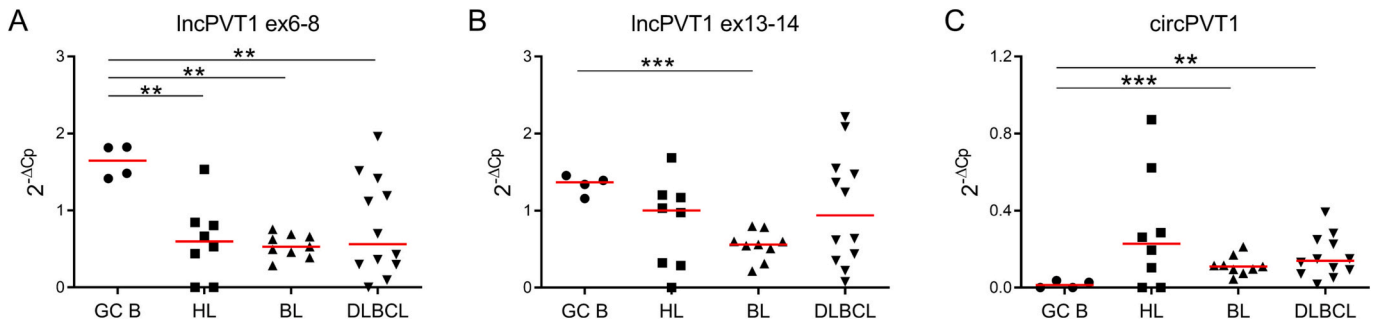

Fig. 1. Expression patterns of linear and circular PVT1 transcripts in B-cell lymphoma cells compared to GC B cells. (A) lncPVT1 transcripts containing exons 6–8; (B) lncPVT1 transcripts containing exons 13–14; (C) CircPVT1 (hsa_circ_0001821) expression levels were determined in 29 B-cell lymphoma cell lines (HL = 8, BL = 9, DLBCL = 12) and 4 GC B cells by RT-qPCR. Relative expression was normalized to TBP and shown as $2^{-\Delta Cp}$. The red line indicates the median. $*p < 0.05$, $**p < 0.01$, $***p < 0.001$. See also supplemental Fig. 1 for details on the exon numbering and primer location. (For interpretation of the references to colour in this figure legend, the reader is referred to the web version of this article.)

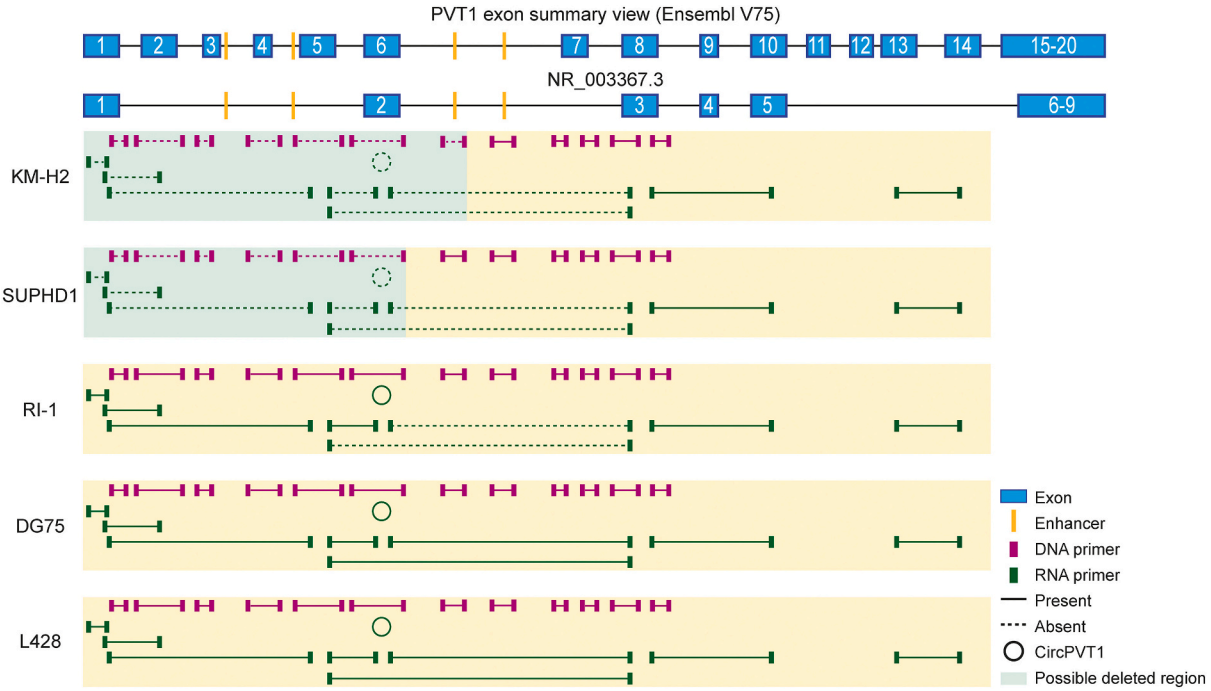

Fig. 2. Analysis of PVT1 deletions in B-cell lymphoma. The PVT1 locus contains 20 possible exons (blue boxes, exon summary view based on Ensemble V75)) and four enhancers; from 5'to 3′ respectively 822E, 866E, 912E, and 919E (orange boxes). For reference, PVT1 refseq NR_003367.3 is shown below the exon summary view. Primers were designed to detect the presence of specific regions in PVT1 at the DNA level (purple boxes) or specific exons at the RNA level (green boxes). The green circle indicates circPVT1 (hsa_circ_0001821). Solid lines indicate a region is present, and dashed lines indicate its absence. The red triangular line between exons indicates that alternative splicing occurs between these two exons. The light green boxes in KM-H2 and SUPHD1 indicate the deleted region we identified. (For interpretation of the references to colour in this figure legend, the reader is referred to the web version of this article.)

3.3. LncPVT1 and circPVT1 knockdown inhibit cell proliferation

To establish a potential role of PVT1 in supporting growth of B-cell lymphoma, we determined the effect of PVT1 knockdown in BL, which is a c-Myc driven malignancy, using GFP competition assays. Approximate locations of the three shRNAs constructs targeting lncPVT1 transcripts and the shRNA targeting the back-splice junction (BSJ) region of circPVT1 are shown in Fig. 3A. LncPVT1 sh1 and sh2 targeting exon 10 showed a moderate knockdown rate of 35 % and 20 % in ST486, respectively. No clear changes in transcript levels were observed for the other two cell lines. In line with the observed knockdown efficiencies, we observed a 25 % and 30 % reduction in the percentage of GFP positive cells in ST486 cells for sh1 for sh2 respectively, while no effects were observed in the other two BL cell lines. LncPVT1 sh3 targeting exon 13 had the best knockdown efficiency (40 % in ST486, 25 % in CA46, and 45 % BL41) and induced an obvious decrease in the percentage of GFP positive cells in all three cell lines (65 % in ST486, 35 % in CA46, 40 % in BL41 at day 22 after infection) (Fig. 3B and C). No clear effects were observed on the expression levels of circPVT1 and MYC upon lncPVT1 knockdown (Supplementary Fig. 6A). The circPVT1 specific BSJ shRNA showed a consistent high knockdown efficiency (85 % in ST486, 70 % in CA46, 90 % in BL41) without affecting the expression of lncPVT1 and MYC (Fig. 3B; Supplementary Fig. 6B). Despite the high efficiency of the shRNA, knockdown of circPVT1 only induced a moderate albeit significant decrease in the percentage of GFP positive cells (30 % in ST486, 12 % in CA46, 28 % in BL41) (Fig. 3D). These data indicates that both circPVT1 and the lncPVT1 transcript containing exons 13–14 support proliferation of BL cells.

Next, we tested the effect of lncPVT1 and circPVT1 knockdown in two HL (L428 and L1236) and two DLBCL (SUDHL5 and SUDHL10) cell

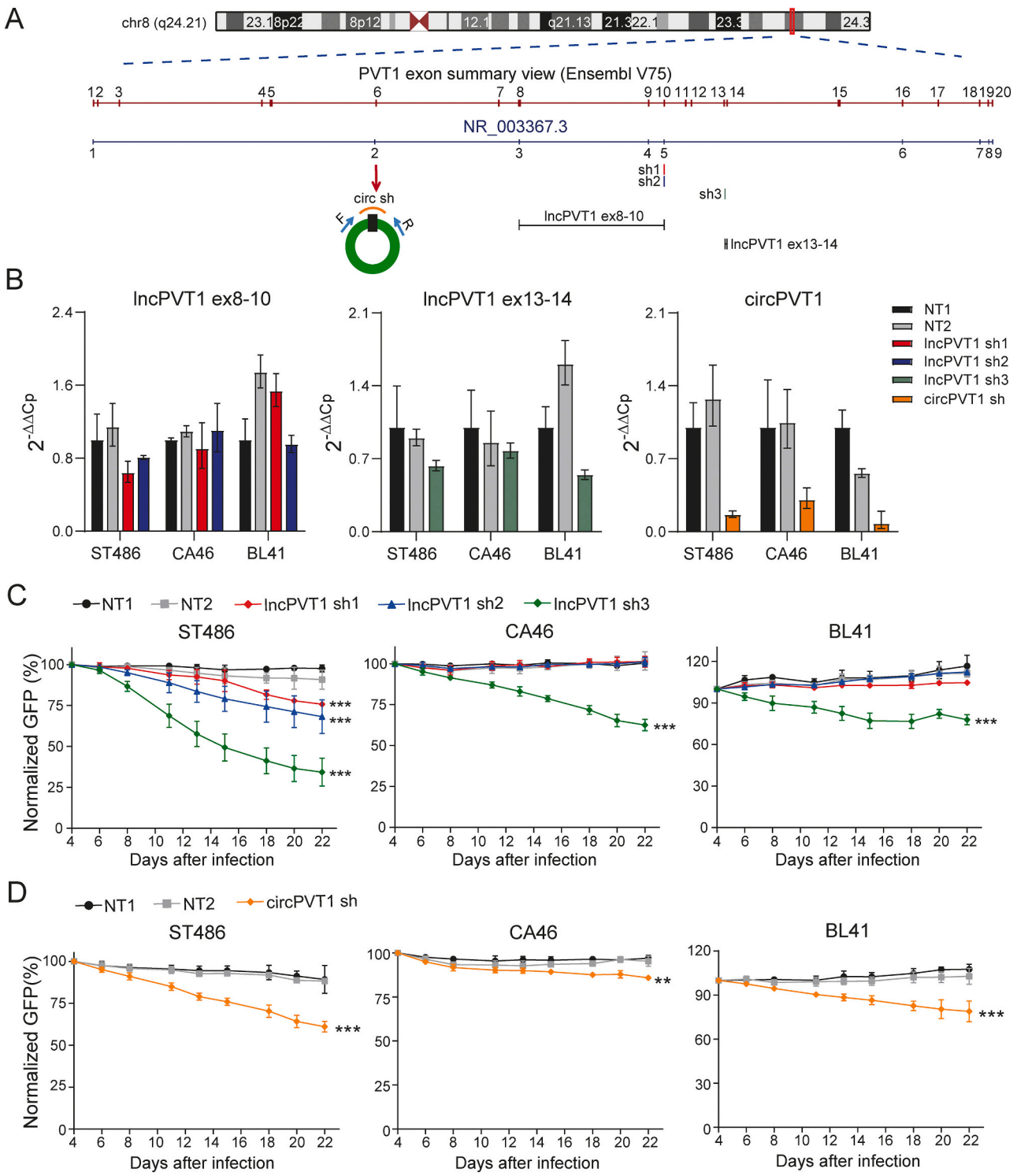

Fig. 3. LncPVT1 and circPVT1 knockdown inhibit cell proliferation. (A) Schematic overview of the PVT1 locus and the location of lncPVT1 and circPVT1 shRNAs and primers used to verify knockdown efficiency. Shown is an exon summary view based on all possible exons reported in Ensemble V75. For reference PVT1 refseq NR_003367.3 is also added. LncPVT1 ex8–10 primer set was used to analyze lncPVT1 sh1 and sh2 efficiency, and lncPVT1 ex13–14 primer set was used to analyze lncPVT1 sh3 efficiency; (B) LncPVT1 and circPVT1 shRNAs knockdown efficiency in ST486, CA46, and BL41 cells. NT1 and NT2 were negative controls. The relative expression was normalized using TBP and calculated as $2^{-\Delta\Delta Cp}$ (NT1 set to 1); (C) LncPVT1 and (D) CircPVT1 knockdown GFP competition assays in ST486, CA46, and BL41 cells. Mean ± SD, $n = 3$. *$p < 0.05$, **$p < 0.01$, ***$p < 0.001$.

lines. LncPVT1 sh3 induced a 35 % decrease in the percentage of GFP positive cells in SUDHL5, whereas no effect was observed in the other three cell lines. Moreover, no effects on the percentage of GFP+ cells were observed for the other shRNAs targeting lncPVT1 in any of the four cell lines (Supplementary Fig. 7A). Knockdown of circPVT1 resulted in a decrease in the percentage of GFP positive cells of 39 % in L1236 but had no effect in L428 and the two DLBCL cell lines (Supplementary Fig. 7B). Thus, in contrast to BL, more variable effects were observed upon lncPVT1 or circPVT1 knockdown in cell lines derived from other B-cell lymphoma subtypes.

3.4. CircPVT1 overexpression promotes cell proliferation

To further study the role of circPVT1, we overexpressed circPVT1 using a lentiviral overexpression vector. The relative increases in circPVT1 levels were most pronounced in KM-H2 and SUPHD1 cells that both harbor a homozygous deletion encompassing the circPVT1 region. For cell lines that already expressed circPVT1 the increases ranged from 3 to 5-fold (Supplementary Fig. 8A). Sequence analysis of the exogenous circPVT1 transcripts showed the expected BSJ sequence (Supplementary Fig. 8B). No effects on MYC expression were observed following circPVT1 overexpression (Supplementary Fig. 8C). The circular shape of the exogenous circPVT1 was confirmed by RT-qPCR on RNase R treated RNA samples (Fig. 4A). Next, we determined the effect of circPVT1 overexpression on cell growth by GFP competition assay in three BL (ST486, CA46, and BL41), four HL (L428, L1236, KM-H2, and SUPHD1), and two DLBCL (SUDHL5 and SUDHL10) cell lines. No changes in the percentage of GFP positive cells were observed in cell lines with high endogenous circPVT1 levels, i.e., all BL and two of the four HL (L428 and L1236) cell lines (Fig. 4B). Slight increases in the percentage of GFP positive cells were observed for the two HL cell lines lacking endogenous circPVT1 and the DLBCL cell lines having a moderate circPVT1 expression, i.e., KM-H2 (20%), SUPHD1 (10 %), SUDHL5 (23 %), and SUDHL10 (20 %) (Fig. 4B). Together, our results suggest that overexpression of circPVT1 has a growth-supporting effect on B-cell

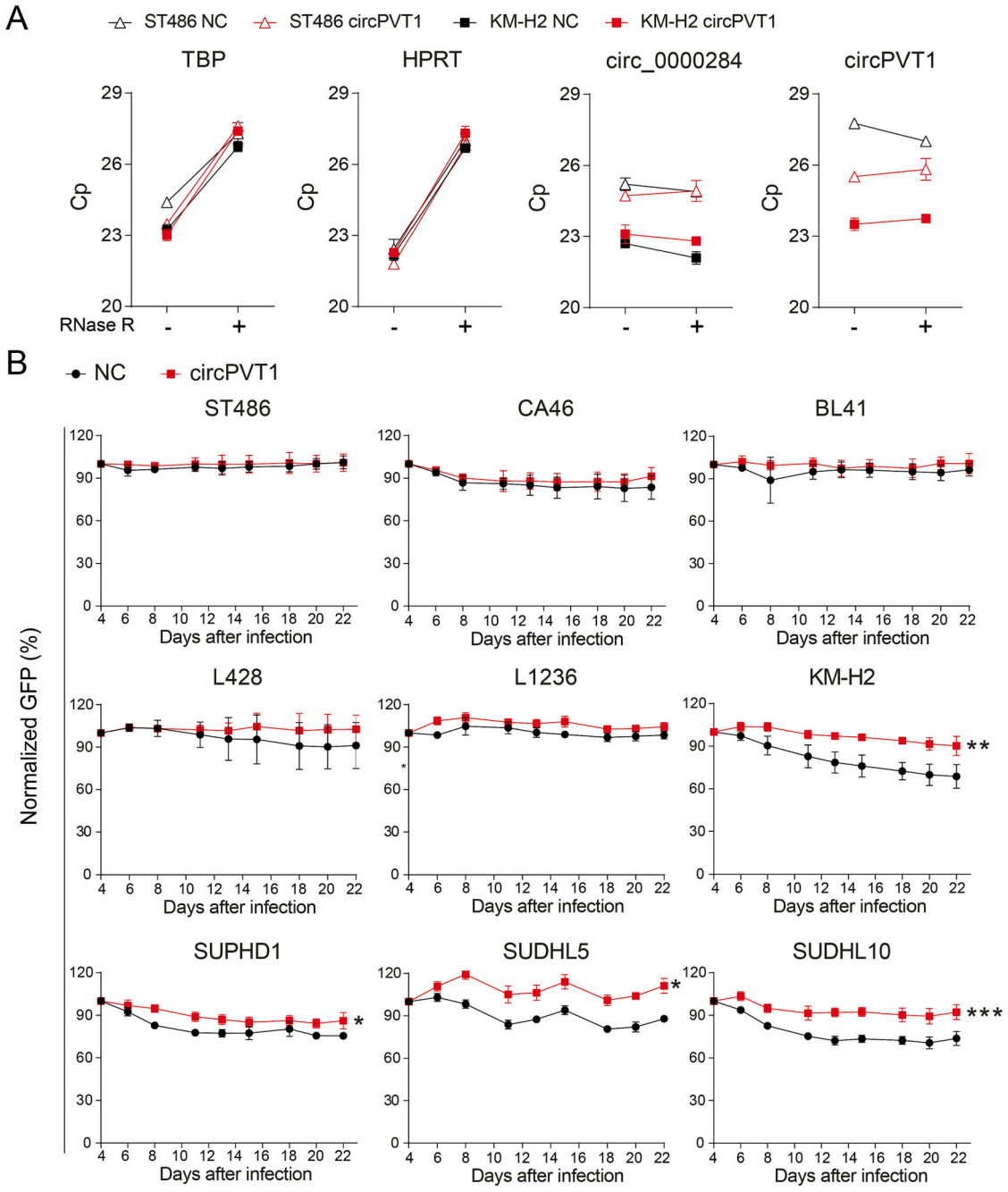

Fig. 4. CircPVT1 overexpression promotes cell proliferation in cell lines with low circPVT1 levels. (A) RNase R treatment to confirm the circular nature of circPVT1 in ST486 and KM-H2 cells overexpressing circPVT1. TBP, HPRT, and circ_0000284 were used as linear and circular controls, respectively. Data were expressed as mean ± SD; (B) circPVT1 overexpression GFP competition assays in 3 BL (ST486, CA46, and BL41), 4 HL (L428, L1236, KM-H2, and SUPHD1), and 2 DLBCL (SUDHL15 and SUDHL10) cell lines. CircPVT1 was not expressed in KM-H2 and SUPHD1 cells. Mean ± SD, n = 3. *$p < 0.05$, **$p < 0.01$, ***$p < 0.001$.

lymphoma cells that lack (KM-H2 and SUPHD1) or have low endogenous (SUDHL5 and SUDHL10) circPVT1 levels.

3.5. No interaction between lncPVT1 or circPVT1 and miRNAs in B-cell lymphoma

The subcellular localization of lncRNAs and circRNAs may provide first hints on their potential functions and regulatory mechanisms. To unravel the potential functional mechanisms of lncPVT1 and circPVT1 transcripts, we analyzed their subcellular localization in nine B-cell lymphoma cell lines (HL = 3, BL = 3, DLBCL = 3). The fransfection efficiency was verified based on the enrichment of U3 and SNHG4 in the nucleus and RPPH1 in the cytoplasm (Fig. 5A). LncPVT1 transcripts were consistently enriched in the nucleus in all 9 cell lines, suggesting that lncPVT1 transcripts may play a role in gene regulation. In contrast, circPVT1 transcripts were enriched in the cytoplasm of the 8 cell lines that expressed circPVT1 (Fig. 5A), suggesting that circPVT1 may interact with miRNA, proteins, mRNAs or be translated into peptides or proteins.

As several studies reported on the interaction of lncPVT1 and circPVT1 with miRNAs in various cancer types [21,42], we focused on establishing potential PVT1-miRNA interactions in B-cell lymphoma. We performed AGO2-RIP in 9 B-cell lymphoma cell lines (HL = 3, BL = 3, DLBCL = 3). AGO2 protein, miRNAs known to be expressed in B-cell lymphoma, and previously confirmed miRNA targets MYLIP and CD69 all showed a good enrichment in the AGO2-IP fractions of all cell lines confirming the effectiveness of the AGO2-RIP procedure (Fig. 5B; Supplementary Fig. 9). However, neither lncPVT1 nor circPVT1 transcripts showed a clear enrichment in the AGO2-IP fraction. We only observed a mild enrichment of lncPVT1 transcripts in the AGO2-IP fraction of KM-H2 and SUDHL10, but not in the other cell lines. Together this indicates that lncPVT1 and circPVT1 do not interact with miRNAs in B-cell lymphoma.

4. Discussion

Linear and circular PVT1 play critical roles in cell proliferation, metastasis, apoptosis, drug resistance, and metabolism in various types of human cancers [16,20,23,25]. In this study, we showed aberrant expression of both lncPVT1 and circPVT1, with lncPVT1 being down and circPVT1 being upregulated in B-cell lymphoma. In addition, we showed a growth-supporting effect of both transcripts. In contrast to what has

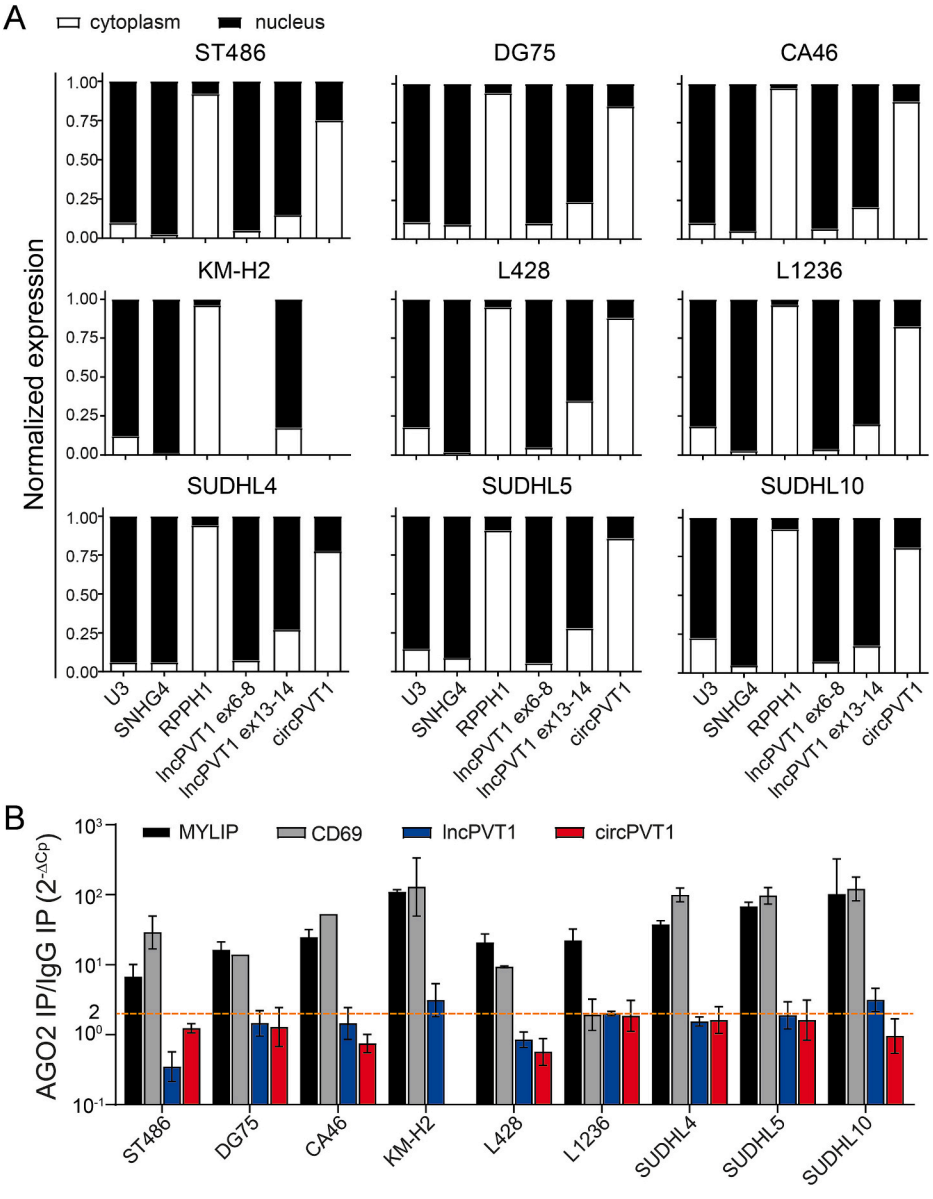

Fig. 5. LncPVT1 and circPVT1 do not interact with miRNAs in B-cell lymphoma. (A) Subcellular localization of lncPVT1 and circPVT1 transcripts in 3 BL (ST486, DG75, CA46), 3 HL (KM-H2, L428, L1236), and 3 DLBCL (SUDHL4, SUDHL5, SUDHL10) cell lines. U3 and SNHG4 were used as nuclear controls, and RPPH1 was used as cytoplasmic control to evaluate the effectiveness of the subcellular localization; (B) AGO2 RNA immunoprecipitation (RIP) assay in 3 BL (ST486, DG75, CA46), 3 HL (KM-H2, L428, L1236), and 3 DLBCL (SUDHL4, SUDHL5, SUDHL10) cell lines shows that in general PVT1 and circPVT1 do not interact with miRNAs in B-cell lymphoma. MYLIP and CD69 were used as positive controls. Relative enrichment was calculated by $2^{-\Delta Cp}$ where ΔCp = Cp (AGO2-IP) – Cp (IgG-IP).

been reported for various other cancer types, our data indicate that these effects of lncPVT1 and circPVT1 in B-cell lymphoma are not dependent on binding to miRNAs.

Previous studies showed that lncPVT1 and circPVT1 are significantly upregulated in many different cancers [23,25]. LncPVT1 expression was shown to be significantly increased in DLBCL tissues as compared to normal lymph node tissues [30,31] and in DLBCL cell lines compared to normal B-lymphoblast-like cell lines [30]. In contrast, we found lower levels of lncPVT1 in B-cell lymphoma cell lines compared to GC B cells using two distinct primer sets amplifying transcripts derived from the 5′ and from the 3′ region of the PVT1 locus. Analysis of normal B-cell subsets revealed higher levels of lncPVT1 transcripts in GC and memory B cells as compared to naïve B-cells. A potential explanation for the observed differences of lncPVT1 expression in published studies and our data might be related to differences in housekeeping genes used for normalization of RT-qPCR data, origin of control samples, and location of the primer sets used to detect lncPVT1 transcripts. To the best of our knowledge, expression of circPVT1 has not been studied in B-cell lymphoma previously. In contrast to the lower levels of lncPVT1, circPVT1 levels were upregulated in B-cell lymphoma compared with GC B cells. GC and memory B cells both showed higher circPVT1 levels than naïve B cells. These results suggest independent mechanisms for the regulation of lncPVT1 and circPVT1 transcription in B-cell lymphoma. Several studies indeed showed that expression of lncPVT1 and circPVT1 are regulated by independent promoters, allowing opposite expression patterns as observed in B-cell lymphoma [28,43,44]. On the other hand, it is also possible that expression differences are (in part) caused by differences in half-life. CircPVT1 is more stable with a half-life exceeding 24 h while the half-life of lncPVT1 is <4 h [45].

Several studies showed intricate relationships between expression of MYC and both linear and circular PVT1. The PVT1 locus is co-amplified with the MYC locus in >98 % of cancers [41]. This co-amplification might explain the strong correlation between MYC and lncPVT1 and circPVT1 transcripts. Moreover, Yang et al. observed a strong positive correlation between lncPVT1 and MYC in 46 DLBCL tissues (Pearson's $r = 0.70$) [31]. In P493–6 B-cells containing a repressible MYC allele, knockdown of MYC resulted in a decrease in the expression of circPVT1 [34]. Knockdown of circPVT1 in B-cell and T-cell acute lymphoblastic leukemia resulted in a decrease of c-Myc levels [35]. We showed a fair correlation (Pearson's r: 0.31–0.48) of lncPVT1 transcripts with MYC expression in B-cell lymphoma. In addition, we observed a weak albeit not significant correlation between circPVT1 and MYC. These correlations were most obvious in MYC translocation negative cell lines. As MYC transcript levels are also high in MYC-translocation negative cell lines, a possible explanation might be that these cell lines have amplifications encompassing MYC and PVT1. Neither knockdown of lncPVT1 or circPVT1 nor overexpression of circPVT1 showed clear effects on MYC expression suggesting that these PVT1 transcripts are not involved in the regulation of MYC in the studied lymphoma cell lines.

Genomic aberrations of the PVT1 promoter region alter the chromatin and topologically associating domains of the PVT1 promoter [28]. These changes can facilitate interactions of the MYC promoter with enhancers at the PVT1 locus and thereby enhance MYC expression [28]. Two studies are in line with these observations. High MYC expression was observed in a case of chronic lymphocytic leukemia with a t(8;13)(q24; q14), with a concomitant loss of the PVT1 locus [46]. Focal deletions of the PVT1 promoter were observed exclusively in double-hit signature DLBCL cases lacking MYC translocations [29]. In this study, we demonstrated deletion of the PVT1 5′ region in two HL cell lines, which may explain the high MYC expression [47].

Overexpression of LncPVT1 significantly promoted proliferation of DLBCL cells in vitro and in mouse xenograft models [30,31]. Knockdown of lncPVT1 in a BL cell line inhibited proliferation through blocking of cell cycle progression [32]. We showed a growth inhibitory effect of lncPVT1 knockdown especially in BL, which is consistent with previous findings. Higher expression of circPVT1 in (highly proliferative) GC B cells vs (mostly quiescent) naïve and memory B cells as shown in our study hints at a proliferation-supportive effect. In addition, we showed that circPVT1 knockdown inhibited growth of all BL cell lines and 1 out of two HL cell lines, while overexpression slightly promoted growth of DLBCL and part of the HL cell lines, suggesting a growth-promoting role of circPVT1 in B-cell lymphoma.

Most studies on linear and circular PVT1 transcripts show that their mechanisms of action is through binding of miRNAs and as such act as competing endogenous RNAs [21,42]. The binding of tumor-suppressive miRNAs to linear and circular PVT1 transcripts results in a relief of oncogenic miRNA targets from miRNA-dependent inhibition. LncPVT1 was recently reported to facilitate DLBCL development by acting as a miR-34b-5p sponge and thereby enhancing Foxp1/β-catenin signaling [30]. In line with the observed almost complete lack of AGO2-IP enrichment of lncPVT1 in our study, we also did not observe expression of miR-34b-5p in a panel of 8 DLBCL cell lines, including the cell lines used in the study (SUDHL6 and U2932) and the cell lines used by us for AGO2-IP (SUDHL4, SUDHL5 and SUDHL10, data not shown). Furthermore, the reported proposed miR-34b-5p sponge function implies that lncPVT1 should be in the cytoplasm, the most common subcellular location of miRNAs. However, we showed that lncPVT1 is predominantly localized in the nucleus. In contrast, we found a predominant cytoplasmic localization for circPVT1 transcripts. Our findings on the subcellular localization are in line with the results shown in gastric cancer in which lncPVT1 was primarily localized in the nucleus and circPVT1 was preferentially localized in the cytoplasm [45]. The difference in subcellular localization increases the likelihood that circPVT1 interacts with miRNAs and makes it less likely that lncPVT1 interacts with miRNAs in B-cell lymphoma. However, we did not find evidence that supports miRNA binding to either lncPVT1 or circPVT1 making it unlikely that they function as competing endogenous RNAs in B-cell lymphoma. In addition to sponging miRNAs, circPVT1 may utilize alternative mechanisms to exert its effects, such as binding to β-TrCP and thereby inhibiting proteasomal degradation of c-Myc [24]. Notably, circPVT1 did not exhibit any protein-coding activity in small cell lung cancer cell line GLC3 [48]. To fully elucidate the functional mechanism of lncPVT1 and circPVT1in B-cell lymphoma, further investigation is necessary, particularly with regards to their interactions with DNA, mRNAs and proteins.

In conclusion, we demonstrated an opposite expression pattern of lncPVT1 and circPVT1 in B-cell lymphoma as compared to GC B cells. The 5' PVT1 region, including circPVT1, was homozygous deleted in two HL cell lines. CircPVT1 promoted growth of three B-cell lymphoma subtypes, whereas lncPVT1 transcripts had the most pronounced effects only in BL. Despite the miRNA binding potency of linear and circular PVT1 as shown in other malignancies, we did not find evidence that these transcripts interact with miRNAs in B-cell lymphoma. Our data indicate a critical role of lncPVT1 in BL and of circPVT1 in three B-cell lymphoma subtypes independent of their miRNA binding potential and highlights the need for further mechanistic studies.

CRediT authorship contribution statement

X.Z. conducted experimental work, performed data analysis and drafted the manuscript. J.K. (Joost Kluiver) and A.v.d.B. designed the study and supervised data analysis and the writing of the manuscript. M. W., J.K. (Jasper Koerts), A.S., D.d.J, B.R., T. v. d. S., and E.B. conducted part of the experimental work. All authors have read and agreed to the published version of the manuscript.

Funding

This work was supported by The Dutch Cancer Society (KWF #10478/2016-1) to AvdB and JK.

Declaration of competing interest

The authors declare the following financial interests/personal relationships which may be considered as potential competing interests: Anke van den Berg and Joost Kluiver obtained financial support provided by the Dutch Cancer Society.

Data availability

All data generated or analyzed during this study are included in the manuscript and/or the supplementary materials.

Appendix A. Supplementary data

Supplementary data to this article can be found online at https://doi.org/10.1016/j.ijbiomac.2023.126744.

References

[1] Finishing the euchromatic sequence of the human genome, Nature 431 (7011) (2004) 931–945.
[2] P. Kapranov, J. Cheng, S. Dike, D.A. Nix, R. Duttagupta, A.T. Willingham, P. F. Stadler, J. Hertel, J. Hackermüller, I.L. Hofacker, I. Bell, E. Cheung, J. Drenkow, E. Dumais, S. Patel, G. Helt, M. Ganesh, S. Ghosh, A. Piccolboni, V. Sementchenko, H. Tammana, T.R. Gingeras, RNA Maps Reveal New RNA Classes and a Possible Function for Pervasive Transcription, Science (New York, N.Y.) vol. 316(5830), 2007, pp. 1484–1488.
[3] J. Cheng, P. Kapranov, J. Drenkow, S. Dike, S. Brubaker, S. Patel, J. Long, D. Stern, H. Tammana, G. Helt, V. Sementchenko, A. Piccolboni, S. Bekiranov, D.K. Bailey, M. Ganesh, S. Ghosh, I. Bell, D.S. Gerhard, T.R., Gingeras, Transcriptional Maps of 10 Human Chromosomes at 5-Nucleotide Resolution, Science (New York, N.Y.) vol. 308(5725), 2005, pp. 1149–1154.
[4] J.K. DiStefano, G.S. Gerhard, Long noncoding RNAs and human liver disease, Annu. Rev. Pathol. 17 (2022) 1–21.
[5] P.J. Batista, H.Y. Chang, Long noncoding RNAs: cellular address codes in development and disease, Cell 152 (6) (2013) 1298–1307.
[6] T.R. Cech, J.A. Steitz, The noncoding RNA revolution-trashing old rules to forge new ones, Cell 157 (1) (2014) 77–94.
[7] A.M. Schmitt, H.Y. Chang, Long noncoding RNAs in cancer pathways, Cancer Cell 29 (4) (2016) 452–463.
[8] A.T. He, J. Liu, F. Li, B.B. Yang, Targeting circular RNAs as a therapeutic approach: current strategies and challenges, Signal Transduct. Target. Ther. 6 (1) (2021) 185.
[9] L.S. Kristensen, T. Jakobsen, H. Hager, J. Kjems, The emerging roles of circRNAs in cancer and oncology, Nat. Rev. Clin. Oncol. 19 (3) (2022) 188–206.
[10] L.L. Chen, L. Yang, Regulation of circRNA biogenesis, RNA Biol. 12 (4) (2015) 381–388.
[11] X. Li, L. Yang, L.L. Chen, The biogenesis, functions, and challenges of circular RNAs, Mol. Cell 71 (3) (2018) 428–442.
[12] H. Suzuki, Y. Zuo, J. Wang, M.Q. Zhang, A. Malhotra, A. Mayeda, Characterization of RNase R-digested cellular RNA source that consists of lariat and circular RNAs from pre-mRNA splicing, Nucleic Acids Res. 34 (8) (2006), e63.
[13] J.U. Guo, V. Agarwal, H. Guo, D.P. Bartel, Expanded identification and characterization of mammalian circular RNAs, Genome Biol. 15 (7) (2014) 409.
[14] C.X. Liu, L.L. Chen, Circular RNAs: characterization, cellular roles, and applications, Cell 185 (12) (2022) 2016–2034.
[15] J. Gearhart, E.E. Pashos, M.K. Prasad, Pluripotency redux–advances in stem-cell research, N. Engl. J. Med. 357 (15) (2007) 1469–1472.
[16] D. Traversa, G. Simonetti, D. Tolomeo, G. Visci, G. Macchia, M. Ghetti, G. Martinelli, L.S. Kristensen, C.T. Storlazzi, Unravelling similarities and differences in the role of circular and linear PVT1 in cancer and human disease, Br. J. Cancer 126 (6) (2022) 835–850.
[17] P. Glažar, P. Papavasileiou, N. Rajewsky, circBase: a database for circular RNAs, Rna 20 (11) (2014) 1666–1670.
[18] F.J. Martin, M.R. Amode, A. Aneja, O. Austine-Orimoloye, A.G. Azov, I. Barnes, A. Becker, R. Bennett, A. Berry, J. Bhai, S.K. Bhurji, A. Bignell, S. Boddu, P.R. Branco Lins, L. Brooks, S.B. Ramaraju, M. Charkhchi, A. Cockburn, L. Da Rin Fiorretto, C. Davidson, K. Dodiya, S. Donaldson, B. El Houdaigui, T. El Naboulsi, R. Fatima, C.G. Giron, T. Genez, G.S. Ghattaoraya, J.G. Martinez, C. Guijarro, M. Hardy, Z. Hollis, T. Hourlier, T. Hunt, M. Kay, V. Kaykala, T. Le, D. Lemos, D. Marques-Coelho, J.C. Marugán, G.A. Merino, L.P. Mirabueno, A. Mushtaq, S.N. Hossain, D.N. Ogeh, M.P. Sakthivel, A. Parker, M. Perry, I. Piližota, I. Prosovetskaia, J.G. Pérez-Silva, A.I.A. Salam, N. Saraiva-Agostinho, H. Schuilenburg, D. Sheppard, S. Sinha, B. Sipos, W. Stark, E. Steed, R. Sukumaran, D. Sumathipala, M.M. Suner, L. Surapaneni, K. Sutinen, M. Szpak, F.F. Tricomi, D. Urbina-Gómez, A. Veidenberg, T.A. Walsh, B. Walts, E. Wass, N. Willhoft, J. Allen, J. Alvarez-Jarreta, M. Chakiachvili, B. Flint, S. Giorgetti, L. Haggerty, G. R. Ilsley, J.E. Loveland, B. Moore, J.M. Mudge, J. Tate, D. Thybert, S.J. Trevanion, A. Winterbottom, A. Frankish, S.E. Hunt, M. Ruffier, F. Cunningham, S. Dyer, R. D. Finn, K.L. Howe, P.W. Harrison, A.D. Yates, P. Flicek, Ensembl 2023, Nucleic acids research 51(D1), 2023, pp. D933–d941.
[19] D. Tolomeo, A. Agostini, G. Visci, D. Traversa, C.T. Storlazzi, PVT1: a long non-coding RNA recurrently involved in neoplasia-associated fusion transcripts, Gene 779 (2021), 145497.
[20] O.T. Onagoruwa, G. Pal, C. Ochu, O.O. Ogunwobi, Oncogenic role of PVT1 and therapeutic implications, Front. Oncol. 10 (2020) 17.
[21] A.C. Palcau, V. Canu, S. Donzelli, S. Strano, C. Pulito, G. Blandino, CircPVT1: a pivotal circular node intersecting Long non-coding-PVT1 and c-MYC oncogenic signals, Mol. Cancer 21 (1) (2022) 33.
[22] J. Adhikary, S. Chakraborty, S. Dalal, S. Basu, A. Dey, A. Ghosh, Circular PVT1: an oncogenic non-coding RNA with emerging clinical importance, J. Clin. Pathol. 72 (8) (2019) 513–519.
[23] S. Ghafouri-Fard, M.D. Omrani, M. Taheri, Long noncoding RNA PVT1: a highly dysregulated gene in malignancy, J. Cell. Physiol. 235 (2) (2020) 818–835.
[24] Y. Mo, Y. Wang, Y. Wang, X. Deng, Q. Yan, C. Fan, S. Zhang, S. Zhang, Z. Gong, L. Shi, Q. Liao, C. Guo, Y. Li, G. Li, Z. Zeng, W. Jiang, W. Xiong, B. Xiang, Circular RNA circPVT1 promotes nasopharyngeal carcinoma metastasis via the β-TrCP/c-Myc/SRSF1 positive feedback loop, Mol. Cancer 21 (1) (2022) 192.
[25] S. Ghafouri-Fard, T. Khoshbakht, M. Taheri, E. Jamali, A concise review on the role of CircPVT1 in tumorigenesis, drug sensitivity, and cancer prognosis, Front. Oncol. 11 (2021), 762960.
[26] A.C. Panda, I. Grammatikakis, K.M. Kim, S. De, J.L. Martindale, R. Munk, X. Yang, K. Abdelmohsen, M. Gorospe, Identification of senescence-associated circular RNAs (SAC-RNAs) reveals senescence suppressor CircPVT1, Nucleic Acids Res. 45 (7) (2017) 4021–4035.
[27] K. Jin, S. Wang, Y. Zhang, M. Xia, Y. Mo, X. Li, G. Li, Z. Zeng, W. Xiong, Y. He, Long non-coding RNA PVT1 interacts with MYC and its downstream molecules to synergistically promote tumorigenesis, Cell. Mol. Life Sci. 76 (21) (2019) 4275–4289.
[28] S.W. Cho, J. Xu, R. Sun, M.R. Mumbach, A.C. Carter, Y.G. Chen, K.E. Yost, J. Kim, J. He, S.A. Nevins, S.F. Chin, C. Caldas, S.J. Liu, M.A. Horlbeck, D.A. Lim, J. S. Weissman, C. Curtis, H.Y. Chang, Promoter of lncRNA gene PVT1 is a tumor-suppressor DNA boundary element, Cell 173 (6) (2018) 1398–1412.e22.
[29] L.K. Hilton, J. Tang, S. Ben-Neriah, M. Alcaide, A. Jiang, B.M. Grande, C. K. Rushton, M. Boyle, B. Meissner, D.W. Scott, R.D. Morin, The double-hit signature identifies double-hit diffuse large B-cell lymphoma with genetic events cryptic to FISH, Blood 134 (18) (2019) 1528–1532.
[30] S. Tao, Y. Chen, M. Hu, L. Xu, C.B. Fu, X.B. Hao, LncRNA PVT1 facilitates DLBCL development via miR-34b-5p/Foxp1 pathway, Mol. Cell. Biochem. 477 (3) (2022) 951–963.
[31] R. Yang, T. Shao, M. Long, Y. Shi, Q. Liu, L. Yang, M. Zhan, Long noncoding RNA PVT1 promotes tumor growth and predicts poor prognosis in patients with diffuse large B-cell lymphoma, Cancer Commun. (London, England) 40 (10) (2020) 551–555.
[32] C. Zheng, Y. Xiao, Y. Li, D. He, Knockdown of long non-coding RNA PVT1 inhibits the proliferation of Raji cells through cell cycle regulation, Oncol. Lett. 18 (2) (2019) 1225–1234.
[33] S. Mizuno, I. Hanamura, A. Ota, S. Karnan, J. Kanasugi, A. Nakamura, S. Takasugi, K. Uchino, T. Horio, M. Goto, S. Murakami, M. Gotou, H. Yamamoto, M. Watarai, M. Shikami, Y. Hosokawa, H. Miwa, M. Taniwaki, R. Ueda, M. Nitta, A. Takami, Establishment and characterization of a novel vincristine-resistant diffuse large B-cell lymphoma cell line containing the 8q24 homogeneously staining region, FEBS Open Bio 8 (12) (2018) 1977–1991.
[34] Q. Gou, K. Wu, J.K. Zhou, Y. Xie, L. Liu, Y. Peng, Profiling and bioinformatic analysis of circular RNA expression regulated by c-Myc, Oncotarget 8 (42) (2017) 71587–71596.
[35] J. Hu, Q. Han, Y. Gu, J. Ma, M. McGrath, F. Qiao, B. Chen, C. Song, Z. Ge, Circular RNA PVT1 expression and its roles in acute lymphoblastic leukemia, Epigenomics 10 (6) (2018) 723–732.
[36] M. Winkle, M.M. Tayari, K. Kok, G. Duns, N. Grot, M. Kazimierska, A. Seitz, D. de Jong, J. Koerts, A. Diepstra, A. Dzikiewicz-Krawczyk, C. Steidl, J. Kluiver, A. van den Berg, The lncRNA KTN1-AS1 co-regulates a variety of Myc-target genes and enhances proliferation of Burkitt lymphoma cells, Hum. Mol. Genet. 31 (24) (2022) 4193–4206.
[37] J. Kluiver, I. Slezak-Prochazka, A. van den Berg, Studying microRNAs in Lymphoma, Methods in Molecular Biology (Clifton, N.J.) vol. 971, 2013, pp. 265–276.
[38] M. Braun, R. Menon, P. Nikolov, R. Kirsten, K. Petersen, D. Schilling, C. Schott, S. Gündisch, F. Fend, K.F. Becker, S. Perner, The HOPE fixation technique–a promising alternative to common prostate cancer biobanking approaches, BMC Cancer 11 (2011) 511.
[39] A. Dzikiewicz-Krawczyk, A. Diepstra, B. Rutgers, G. Kortman, D. de Jong, J. Koerts, M. Bulthuis, T. van der Sluis, A. Seitz, L. Visser, K. Kok, J. Kluiver, A. van den Berg, Argonaute 2 RNA immunoprecipitation reveals distinct miRNA Targetomes of primary Burkitt lymphoma tumors and normal B cells, Am. J. Pathol. 188 (5) (2018) 1289–1299.
[40] Y. Yuan, J. Kluiver, J. Koerts, D. de Jong, B. Rutgers, F.R. Abdul Razak, M. Terpstra, B.E. Plaat, I.M. Nolte, A. Diepstra, L. Visser, K. Kok, A. van den Berg, miR-24-3p is overexpressed in Hodgkin lymphoma and protects Hodgkin and Reed-Sternberg cells from apoptosis, Am. J. Pathol. 187 (6) (2017) 1343–1355.
[41] Y.Y. Tseng, B.S. Moriarity, W. Gong, R. Akiyama, A. Tiwari, H. Kawakami, P. Ronning, B. Reuland, K. Guenther, T.C. Beadnell, J. Essig, G.M. Otto, M. G. O'Sullivan, D.A. Largaespada, K.L. Schwertfeger, Y. Marahrens, Y. Kawakami, A. Bagchi, PVT1 dependence in cancer with MYC copy-number increase, Nature 512 (7512) (2014) 82–86.
[42] W. Wang, R. Zhou, Y. Wu, Y. Liu, W. Su, W. Xiong, Z. Zeng, PVT1 promotes cancer progression via MicroRNAs, Front. Oncol. 9 (2019) 609.

[43] M. Ghetti, I. Vannini, C.T. Storlazzi, G. Martinelli, G. Simonetti, Linear and circular PVT1 in hematological malignancies and immune response: two faces of the same coin, Mol. Cancer 19 (1) (2020) 69.
[44] L. Verduci, M. Ferraiuolo, A. Sacconi, F. Ganci, J. Vitale, T. Colombo, P. Paci, S. Strano, G. Macino, N. Rajewsky, G. Blandino, The oncogenic role of circPVT1 in head and neck squamous cell carcinoma is mediated through the mutant p53/YAP/TEAD transcription-competent complex, Genome Biol. 18 (1) (2017) 237.
[45] J. Chen, Y. Li, Q. Zheng, C. Bao, J. He, B. Chen, D. Lyu, B. Zheng, Y. Xu, Z. Long, Y. Zhou, H. Zhu, Y. Wang, X. He, Y. Shi, S. Huang, Circular RNA profile identifies circPVT1 as a proliferative factor and prognostic marker in gastric cancer, Cancer Lett. 388 (2017) 208–219.
[46] G. Macchia, A. Lonoce, S. Venuto, E. Macrí, O. Palumbo, M. Carella, C. Lo Cunsolo, P. Iuzzolino, M. Hernández-Sánchez, J.M. Hernandez-Rivas, C.T. Storlazzi, A rare but recurrent t(8:13)(q24;q14) translocation in B-cell chronic lymphocytic leukaemia causing MYC up-regulation and concomitant loss of PVT1, miR-15/16 and DLEU7, Br. J. Haematol. 172 (2) (2016) 296–299.
[47] L. Ziel-Swier, Y. Liu, A. Seitz, D. de Jong, J. Koerts, B. Rutgers, R. Veenstra, F.R. A. Razak, A. Dzikiewicz-Krawczyk, A. van den Berg, J. Kluiver, The role of the MYC/miR-150/MYB/ZDHHC11 network in Hodgkin lymphoma and diffuse large B-cell lymphoma, Genes 13 (2) (2022).
[48] D. Tolomeo, D. Traversa, S. Venuto, K.K. Ebbesen, J.L. García Rodríguez, G. Tamma, M. Ranieri, G. Simonetti, M. Ghetti, M. Paganelli, G. Visci, A. Liso, K. Kok, L.A. Muscarella, F.P. Fabrizio, M.A. Frassanito, A. Lamanuzzi, I. Saltarella, A.G. Solimando, A. Fatica, Z. Ianniello, R.M. Marsano, A. Palazzo, A. Azzariti, V. Longo, S. Tommasi, D. Galetta, A. Catino, A. Zito, T. Mazza, A. Napoli, G. Martinelli, J. Kjems, L.S. Kristensen, A. Vacca, C.T. Storlazzi, circPVT1 and PVT1/AKT3 show a role in cell proliferation, apoptosis, and tumor subtype-definition in small cell lung cancer, Gene Chromosome Cancer 62 (7) (2022) 377–391.